

## Understanding the Design and Control of VSC-Based HVDC System with Shunt Passive Filters

Banishree Misra<sup>1</sup>, Byamakesh Nayak<sup>2</sup>

<sup>1,2</sup> School of Electrical Engineering, KIIT University, Bhubaneswar, India.

### Abstract

A detail description of the operating scheme of a 12-pulse voltage source converter (VSC) used in high voltage DC (HVDC) system is presented here. The system used here for HVDC transmission schemes comprises only one terminals with a 12-pulse converter and a DC load of 1000MW. Then the design of the control structure for the triggering circuit and the technique of pulse generation for the thyristor based converter is explained and analysed using MATLAB/SIMULINK. The effect of changing the firing pulse on the active and reactive power generation and the total harmonic distortion of the source current is investigated. The simulation results confirms the capability of HVDC converter operating with a wide range of firing angles. The parameters of different passive harmonic filters are calculated. The harmonic study of the VSC based HVDC system with shunt passive filters confirms the effectiveness of the filters. All the results are validated in MATLAB/SIMULINK environment.

**Keywords:** VSC based HVDC system; 12-pulse converter; phase locked loop; passive filter; reactive power; total harmonic distortion.

### INTRODUCTION

The concept on which an HVDC system operates is the conversion of generating current from AC to DC (rectification) at the transmitting end, and from DC to AC (inversion) at the receiving end. Using the following converters the target can be achieved [1]-[4]:

1. Thyristor based line-commutated current-source converters (CSCs). (Fig. 1, CSC-HVDC). These converters are well applied for high power applications, usually in the order of 1000MW.
2. Fully controllable switch based forced-commutated voltage-source converters (VSCs). These converters uses mostly gate-turn-off thyristors (GTOs) or for industrial application insulated gate bipolar transistors (IGBTs) (Fig. 2, VSC-HVDC). This technology is mostly used for medium power level in the range of 350MW.

The main difference between CSCs and VSCs is that the VSCs are able to control the active and reactive power injections independent from each other as well as from the system state whereas CSC can control the active power only. With the CSC the DC current polarity will remain the same and hence the power flow direction through the converter is decided by the polarity of the DC voltage. Semi-controllable thyristors are the building blocks for the current source converters. The triggering pulse of the thyristors will decide the instant at

which the current starts conduction. However the the device commutation instant is calculated by the natural zero crossing of the AC voltage. A large smoothing reactors is connected in series at the DC terminal of a CSC to keep the current smooth and continuous [5]-[7]. The total harmonic distortion of the voltage and current is calculated on the AC side. To eliminate the harmonic content large passive and active filters are designed. On the contrary, the voltage source converter VSC do not change the polarity of the DC voltage, so the power flow direction is determined by the polarity of the DC current. These converters are equipped with fully controllable semiconductor switches such as IGBTs. Here the conduction and commutation of the current at any instant is decided by a gate pulse. Like a voltage source, the DC terminal of a VSC is joined in parallel with a comparatively large capacitor.

Both these converter technologies have their own advantages hence used in different power system applications. One of the common application is being the compensation. Here compensation will be made by a power-electronic compensator which will increase the power transfer capability of the line, will increase the efficiency of the power transfer, will improve voltage and angle stability and ultimately will improve the power quality. A HVDC converter controls power on the DC link and at the same time execute certain other tasks. For example it makes a balance between the frequency, voltage magnitude or power factor, of the system. Fig. 1. provides a structural difference of the two converter technologies.

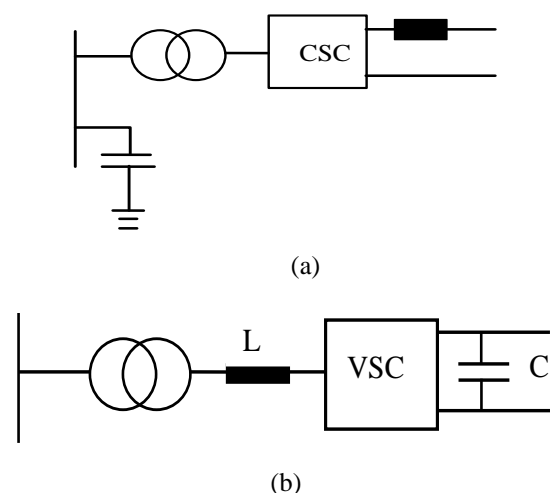


Figure 1. Comparison of (a) CSC and (b) VSC configuration

**COMPONENTS OF VSC-BASED HVDC SYSTEM WITH 12-PULSE AC-DC CONVERTER**

*A. Three Phase Source*

In the proposed HVDC system the source is balanced three-voltage source with an internal R-L impedance. The three phase voltage sources are connected in Y with the neutral internally grounded. The internal resistance is considered zero while the inductance is taken as 98.03 ohm. The design has been considered for a 60 Hz supply system. The AC supply systems is demonstrated by damped L-R equivalents with an angle of 80 degrees at fundamental frequency 60 Hz.

*B. Thyristor Controlled Rectifier*

The schematic diagram of 12-pulse converter based HVDC system with a 1000 MW (500kV and 2 kA) load is shown in Fig. 1. The 12-pulse converter consist of two series connected thyristor bridges connected with a three-phase converter transformer. The thyristor bridges is a universal three-phase power converter which consists of six power switches connected in a bridge configuration. The universal Bridge block is the basic block for designing two-level voltage-sourced converters (VSC). Observing from the AC side, an HVDC converter acts as a source of harmonic currents. The harmonic order is decided on the basis of the number of pulses p generated by the converter section. For the AC side the current harmonics will have a order of  $n = kp \pm 1$ , where k can be any integer. So for a 6-pulse converter considering p = 6, the injected current harmonics on the AC side will have the order of 5,7,11,13.

*C. Three Phase Three Winding Transformer*

The required phase shift between the two set of voltages is 30° (360°/ Total number of pulses) can be generated if the converter is connected to a Y-Δ connected secondary of a transformer. The primary of the transformer is a Y-connection with grounded neutral(winding-1) and on the secondary the winding-2 is Y connected and winding-3 is Δ(D1) connected. so the winding-3(D1) is lagging winding-2 (Y) by an angle of 30 degrees.

**CONTROL SCHEME FOR VSC BASED HVDC SYSTEM**

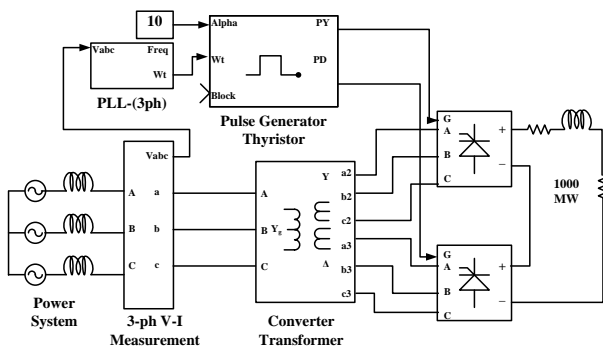


**Figure 2.** Block diagram showing pulse generator block connected to a twelve-pulse thyristor converter.

The firing pulses for the two series connected three-phase thyristor bridge will be generated by the pulse generator. The set of pulses for each converter contains six equally placed square pulses with 60° phase displacement between them. The Py set of pulses will be applied to the first converter bridge connected to the Y-connected secondary winding of the three-phase three winding converter transformer. The Pd set of pulses will go to the Δ-connected secondary winding of the three winding transformer.

The Pulse Generator of the 12-pulse thyristor converter can be controlled by the reference signal (alpha angle) and by the synchronization parameter  $\omega_t$ . It is an angle varying between 0 and 360°. The  $\omega_t$  signal is synchronized with the zero crossing of the fundamental voltage of phase A (positive sequence) of the primary side of the three phase three winding transformer. The information about  $\omega_t$  signal can be obtained from the phase locked loop (PLL) system.

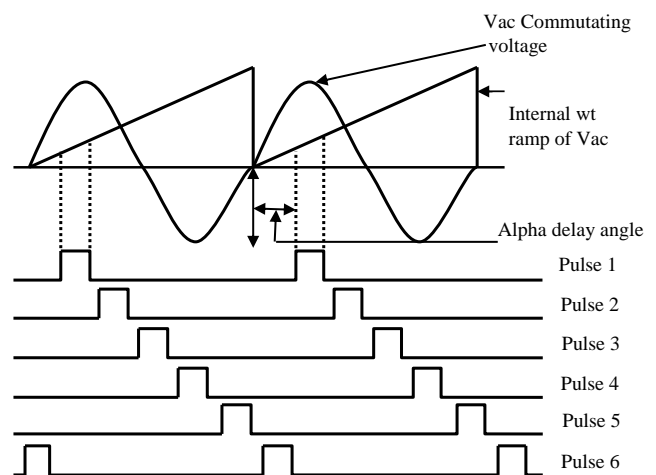


**Figure 3.** PY and PD pulse train generation technique

An internal  $\omega_t$  ramp signal is generated by the pulse generator block which will control the instant of pulse generation. The angle alpha in electrical degrees is the delay by which the pulse is delayed with respect to the angle zero of its fundamental commutating voltage. The generation technique of pulse train Py can be explained corresponding to Fig. 4. In this the thyristor pulse generator is configured to generates two pulse trains simultaneously. At an delay angle of alpha the first pulse is generated and exactly after 60° the second pulse will reach the second converter bridge.

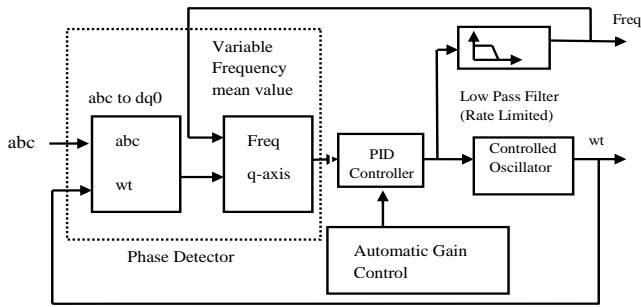


Figure 4. Internal diagram of the 3-phase lock loop

The internal diagram of the three-phase lock loop confirms it to be a closed loop system where the frequency and phase of the sinusoidal three phase signal can be tracked using a frequency oscillator.

In Fig. 4 the phase lock loop building block models closed-loop control system. It tracks the phase and frequency of a three-phase sinusoidal signal by means of an internal frequency oscillator. The close loop control system regulates the internal oscillator frequency to maintain the phases difference to 0. The sinusoidal three-phase input signal is converted to dq0 synchronously rotating reference frame (Park transform) using the angular speed of an internal oscillator. The quadrature axis (q-axis) of the signal, proportional to the phase difference between the abc signal and the internal oscillator rotating frame, is filtered with a Mean (Variable Frequency) block. A Proportional-Integral-Derivative (PID) controller, with an optional automatic gain control (AGC), keeps the phase difference to 0 by acting on a controlled oscillator. The output of PID, corresponding to the angular velocity, is filtered out and transformed to the frequency, in hertz, which is used by the mean value. Fig. 4. shows the detail diagram of the Phase Lock Loop (PLL).

PERFORMANCE EVALUATION OF THE 12-PULSE HVDC AC-DC CONVERTER

A. System Without Filter (1000MW resistive load)

In the present work a VSC based HVDC system is designed in the MATLAB/Simulink background, and its performance is

analysed for 1000MW load with resistive load. The system has been simulated without filters and with filters to study the total harmonic distortion. Rated active power demand is 1000MW, line voltage (VL): 500kV with 60 Hz supply frequency. The source current and voltage waveforms for a firing angle delay of 10° is given in Fig. 6. The pulse train PY and PD for the thyristor converters are given in Fig. 5. The performance of the system is evaluated on the basis of various parameters such as THD content in source voltage & current, the active and reactive power demand on the source side for various values of firing angle, the percentage of reactive power demand with respect to the total apparent power. All these values are given in table I and II for reference.

For a firing angle  $\alpha = 0^\circ$ , three phase reactive power demand is approximately 280 MVAR. Therefore, to provide this reactive power demand for elimination of the harmonics of order 5<sup>th</sup>, 7<sup>th</sup>, 11<sup>th</sup> and 13<sup>th</sup>, suitable passive filters can be designed. Since the load contains 12-pulse converters, 11<sup>th</sup> and 13<sup>th</sup> order harmonics will have the dominant values as calculated in table I. The pattern of increase and decrease of reactive power as a % of total apparent power is given in Table II. for different values of firing angle. From Table I & II it is clear that for a firing angle above 45° the reactive power demand is increasing in nature where as above 90° it becomes nearly constant.

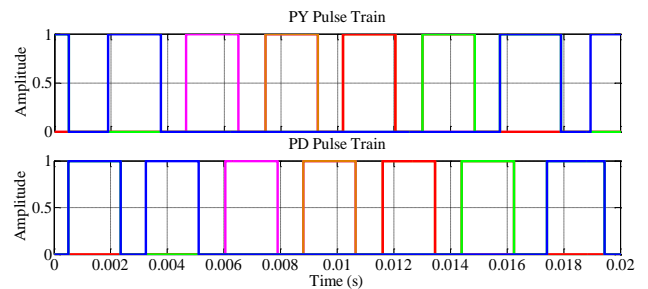


Figure 5. Simulated PY and PD pulse train

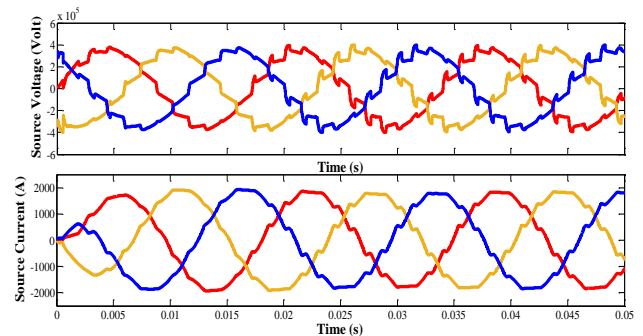


Figure 6. Three phase source voltage and source current signals

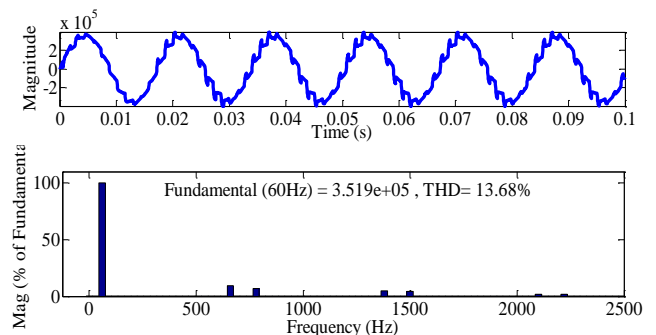


Figure 7. Harmonic spectrum for source voltage

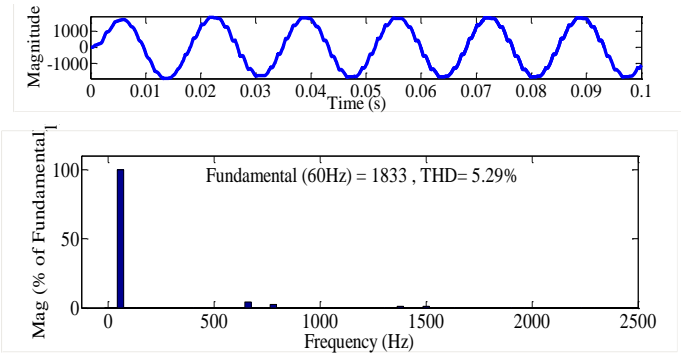


Figure 8. Harmonic spectrum for source current

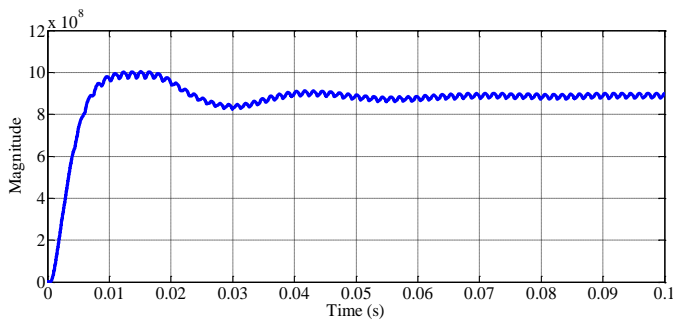


Figure 9. Output DC power without Passive Filter

Table I: Harmonic profile of source current for different values of firing angle of thyristor converter

Thyristor Firing Angle ( $\alpha^0$ )	MVAR (Q)	MW (P)	Harmonics in source current				
			$h_5$ (%)	$h_7$ (%)	$h_{11}$ (%)	$h_{13}$ (%)	THD (%)
$0^0$	280.2	983.6	0.05	0.03	2.47	1.31	2.91
$10^0$	369.3	901.8	0.04	0.01	4.25	2.59	5.20
$20^0$	695.9	769.8	0.07	0.05	6.17	4.30	7.63
$30^0$	637.9	716.3	0.06	0.09	7.9	5.66	7.39
$40^0$	353.1	562.4	0.11	0.06	9.32	6.7	9.78
$50^0$	309.7	331.9	0.14	0.17	10.51	7.51	11.64
$70^0$	387.6	124.8	0.65	0.25	13.83	8.15	17.57
$90^0$	-3.425	2.521	2.07	1.58	78.6	5.49	87.57
$120^0$	-4.515	3.524	1.53	1.47	98.52	93.57	158.58

Table II: Total Reactive Power Demand as a Percentage of Total Apparent Power

Thyristor Firing Angle ( $\alpha^0$ )	MVAR (Q)	MW (P)	MVA	% of MVAR
$0^0$	280.2	983.6	1022.73	27.39
$10^0$	369.3	901.8	974.48	37.89
$20^0$	695.9	769.8	1037.72	67.02
$30^0$	637.9	716.3	959.16	66.50
$40^0$	353.1	562.4	664.05	53.17
$50^0$	309.7	331.9	453.95	68.22
$70^0$	377.6	124.8	397.68	94.95
$90^0$	-3.425	2.521	4.2527	80.53
$120^0$	-4.515	3.524	5.7274	78.83

### PASSIVE HARMONIC FILTER DESIGN FOR VSC BASED HVDC SYSTEM

Conventional Passive Filters with (1000MW resistive load)

The conventional passive filters used for harmonic elimination consist of inductors, capacitors and resistors. They are categorized as high-pass or band-pass filters and tuned filters. In a shunt configuration of VSC based HVDC system these filters are connected in parallel with nonlinear loads such as uncontrolled/controlled rectifiers, fluorescent lamps, or electric arc furnaces. Taking the VSC based HVDC system with the same DC load into consideration here three passive filters are designed of total reactive power rating of 600 Mvar [11]. First one is a C-type filter tuned to the 3<sup>rd</sup> harmonic frequency, second one is a double-tuned filter tuned to 11<sup>th</sup> and 13<sup>th</sup> harmonic frequency and last one is a second order high-pass filter tuned to the 24<sup>th</sup> harmonic frequency [12]. The filter configurations are given in Fig 10. All the filter parameters are calculated and provided in Table III [13]-[14]. The complete configuration of VSC based HVDC system is provided in Fig. 11.

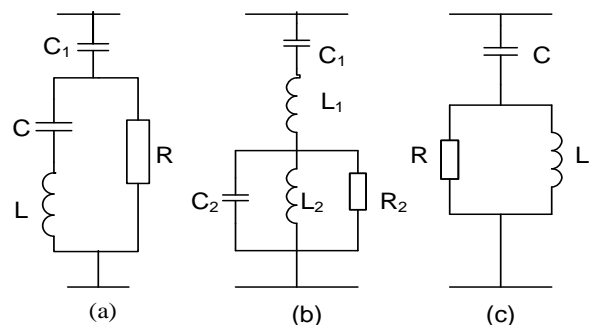


Figure 10. Passive filters (a) C-type filter, (b) double tuned filter, and (c) second order high pass filter

1) C-Type Passive Filter Design

The parameters of the C-type filter as shown in Fig. 10 (a) can be derived and evaluated as shown in the following equations [15].

The C-Type filter capacitance  $C_1$  can be found out from the fundamental harmonic relation:

$$Q_F = -\frac{U^2}{Im(Z_F(\omega_1))} \Rightarrow C_1 = \frac{Q_F}{\omega_1 U^2} \quad (1)$$

The resonance angular frequency of C-type filter is calculated as

$$\omega_r = n_r \omega_1 \quad (2)$$

Where the resonant angular frequency is  $\omega_r$ , order of the resonant frequency is  $n_r$ , and the fundamental harmonic angular frequency is  $\omega_1$ .

For C-type filter  $L_2$  and  $C_2$  are tuned to the fundamental frequency. The parameter  $C_2$  and  $L_2$  can be found out as

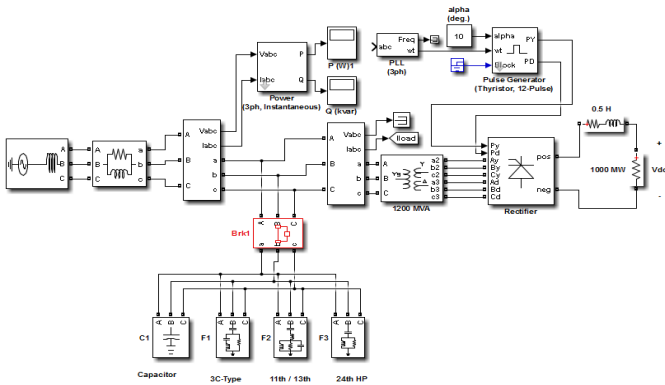


Figure 11. VSC based HVDC system with passive filter

$$\omega_r = \frac{1}{\sqrt{L_2 \frac{C_1 C_2}{C_1 + C_2}}} \Rightarrow C_2 = C_1 (n_r^2 - 1) \quad (3)$$

And

$$L_2 = \frac{1}{\omega_1^2 + C_2} \quad (4)$$

$$R_T = \frac{U^2}{n_r^3 Q_F^2 k \omega_1 L_s} \sqrt{U^4 - n_r^4 Q_F^2 k^2 \omega_1^2 L_s^2} \quad (5)$$

Where,

Operating voltage of the filter capacitor is  $U$ , filter capacitive reactive power  $Q_F$ , impedance of the filter is  $Z_F$ , network inductance  $L_s$ , co-efficient  $k$  whose value is decided according to the percentage distribution of harmonic current between the filter tuned to that harmonic and supply network.

2) Double Tuned Passive Filter Design

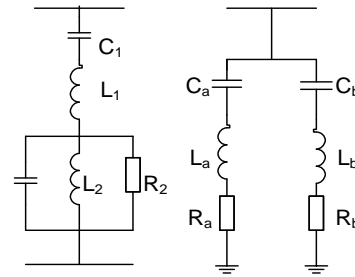


Figure 12. The arrangement of two single tuned filters and a double tuned filter

For simplification of calculation, a double tuned filter is considered to be comparable to two single-tuned filters connected as above in Fig. 12[16]. The double tuned filter parameters can be calculated in terms of the parameters of two single tuned filters. Neglecting the resistance in the filter design, all the parameters of the double tuned filter are calculated as given below.

$$C_a = \frac{Q_F (n_r^2 - 1)}{\omega n_r^2 U^2} \quad (6)$$

$$L_a = \frac{1}{\omega^2 n_r^2 C_a} \quad (7)$$

For the calculation of parameters of a double tuned filter

$$C_1 = C_a + C_b \quad (8)$$

$$L_1 = \frac{L_a L_b}{L_a + L_b} \quad (9)$$

$$C_2 = \frac{C_a C_b (C_a + C_b) (L_a + L_b)^2}{(C_a L_a - C_b L_b)^2} \quad (10)$$

$$L_2 = \frac{(C_a L_a - C_b L_b)^2}{(C_a + C_b)^2 (L_a + L_b)} \quad (11)$$

If the fundamental rated voltage of the network is  $U$ , and at fundamental frequency the impedance of the filter is  $Z_F$ , the fundamental reactive power supplied by the filter  $Q_F$  is given by

$$Q_F = -\frac{U^2}{Z_F} \quad (12)$$

3) Damped Second Order High Pass Filter

The typical arrangement of a damped high-pass filter is shown in Fig. 10 (c). The capacitive and reactive reactance and the resistance can be determined from the following equations [17].

$$X_C = \frac{U^2}{Q_F} \quad (13)$$

Reactor reactance to trap the  $n_r$  th harmonic will have the value of

$$X_L = \frac{X_C}{n_r^2} \quad (14)$$

$$R = X_n Q, \quad R = X_L n_r Q \quad (15)$$

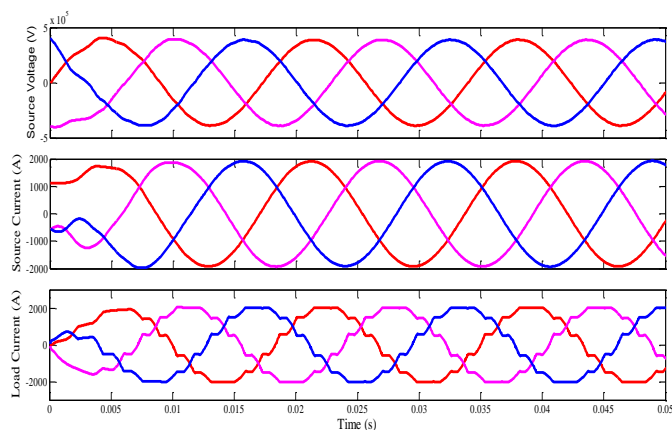
The filter size can be found out in terms of the reactive power generated at fundamental-frequency

$$Q_F = \frac{U^2}{X_C - X_L} \quad (16)$$

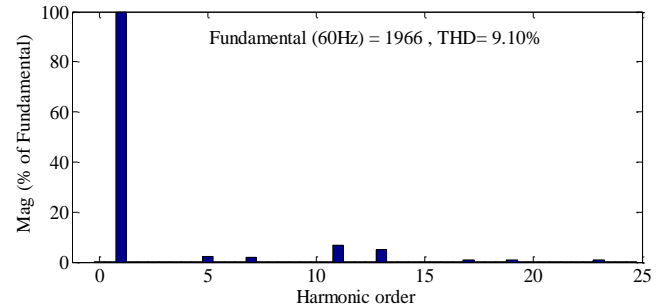
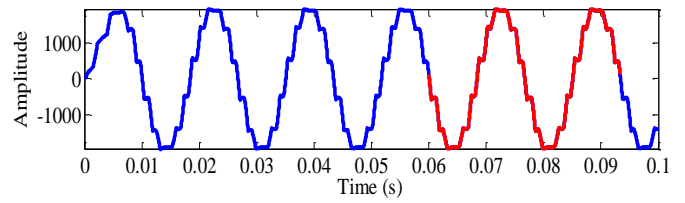
**Table III:** Parameters of the Passive Filter Configuration

Operating voltage of the AC network (kV)					500
Frequency (Hz)					60
Each Branch Size (MVar)					150
Branch Type	Tuning Harmonic	Quality Factor	L (mH)	C (μF)	R (Ω)
C-Type High Pass	3	2	550	C <sub>1</sub> = 1.59 C = 12.7	1111.11
Double Tuned	11, 13	20	L <sub>1</sub> = 15.2 L <sub>2</sub> = 0.46	C <sub>1</sub> = 3.15 C <sub>2</sub> = 107	2740
High Pass	24	7	7.67	1.59	486

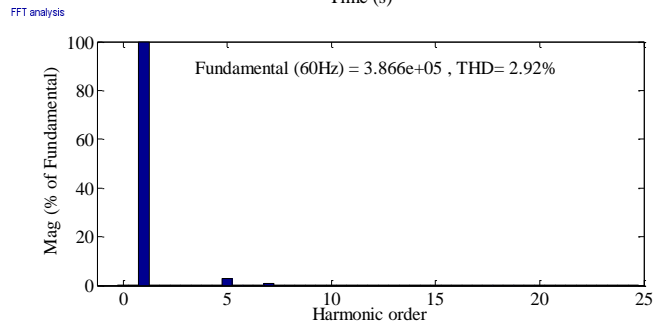
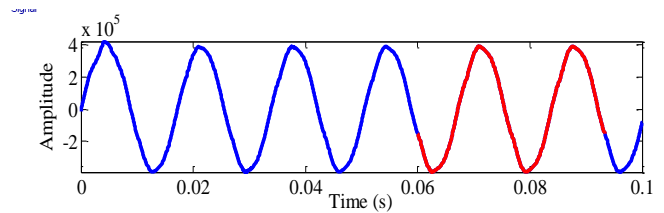
4) Simulation Results



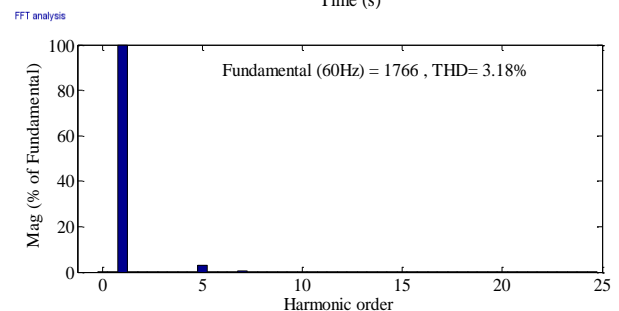
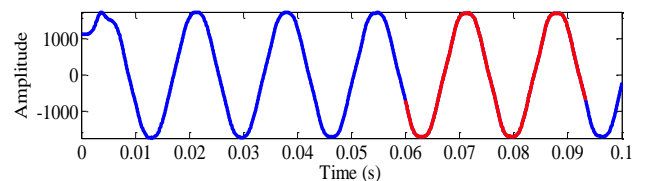
**Figure 13.** AC source voltage, source current & load current waveforms with passive filter.



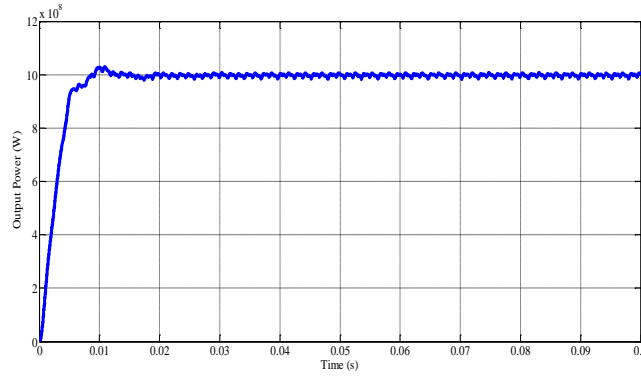
**Figure 14.** Harmonic spectrum of load current with passive filter.



**Figure 15.** Harmonic spectrum of source voltage with passive filter.



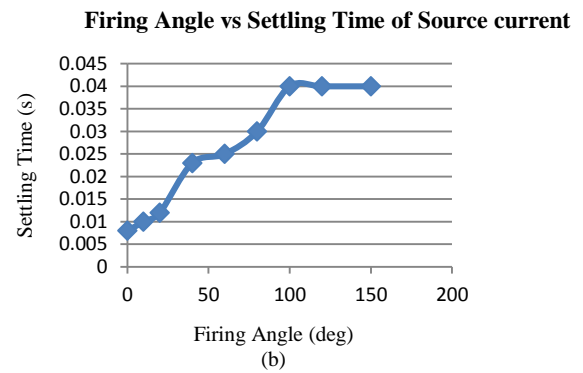
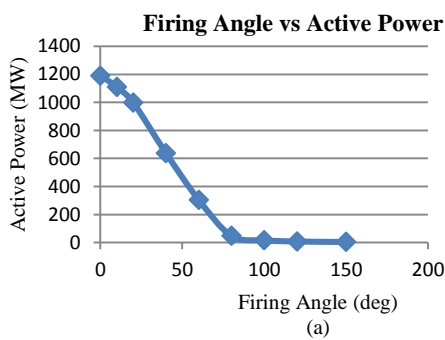
**Figure 16.** Harmonic spectrum of source current with passive filter.



**Figure 17.** Output DC power with Passive Filter

**Table IV:** Performance Analysis of Passive Filters used for Vsc Based HvdC System

Thyristor Firing Angle ( $\alpha^0$ )	Reactive Power MVAR (Q)	Active Power MW(P)	Settling Time of Source Current (s)	THD (Source Current)
0 <sup>0</sup>	-171	1191	0.008	0.4%
10 <sup>0</sup>	-93.1	1110	0.010	0.58%
20 <sup>0</sup>	-15.7	999	0.012	0.83%
40 <sup>0</sup>	83.7	638	0.023	0.85%
60 <sup>0</sup>	-27.3	305	0.025	1.17%
80 <sup>0</sup>	-502	48	0.030	0.63%
100 <sup>0</sup>	-762	16.7	0.04	0.3%
120 <sup>0</sup>	-768	8.31	0.04	0.21%
150 <sup>0</sup>	-778	4.46	0.04	0.16%





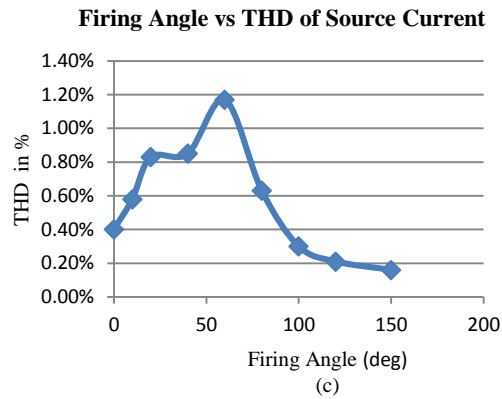


**Figure 18.** Representation of variation of (a) active power, (b) settling time and (c) THD of source current with the triggering angle of thyristor converter.

When shunt passive filter is connected in the VSC based HVDC system, the waveforms of the source current and source voltage are significantly improved due to compensation of the distortions present in the load current. Fig 14 shows the total harmonic distortion in the load current and Fig. 15 & Fig. 16 shows the improvement in the harmonic spectrum of the source current and source voltage with the use of filters. The THD in the source voltage waveform for a DC load of 1000 MW is found to be 2.92% and the THD in the source current waveform is found to be 3.18% which are within the IEEE standard limit. As seen from Fig. 17, the DC output power is also drastically improved after connection of the passive filters. Hence the power balancing effect of the load is reasonable and the system performance is better with the use of passive filters as compared to the system without any filter.

The details of the performance analysis of VSC based HVDC system with passive filters is provided in Table IV. In Fig. 18 the variation of active power, settling time and THD of source current with the triggering angle of thyristor converter is shown. From the analysis of the graphs it is clear that with increase in firing angle the active power demand reduces while the settling time of the source current waveform increases. The total harmonic distortion of the source current lies within the specified International Standard IEEE-519 limit for any value of firing angle. As observed from the performance analysis provided in Table IV, the required power output at the load can be obtained at a firing angle of about  $20^\circ$ . As observed passive filters are not suitable for variable loads as they are designed for specific tuning frequency and specific reactive power.

## CONCLUSION

In this paper a complete operational idea about the VSC based HVDC system has been presented. A detail analysis is made for various components of the system like the converter transformers, pulse generators for the thyristors and the three-phase PLLs. The system has been analysed with different harmonic components and the total harmonic distortion has been calculated for different firing angle. On the basis of the

simulation results of the three phase HVDC system without filters, a complete data analysis has been made to show the total reactive power demand for different firing angles of the converter. With the help of the reactive power demand, the parameters of the passive filters are calculated, then the system has been designed with the passive filters in MATLAB/SIMULINK environment. With the shunt passive filters connected, the system improves the quality of power injected into the DC load at the required firing angle. The results have been analysed and the robustness of the system can be determined from the harmonic analysis of the source current. For the given reactive power demand, the simulation results are providing satisfactory operation of the passive filters.

## REFERENCES

- [1] D. Tiku, "dc Power Transmission: Mercury-Arc to Thyristor HVdc Valves [History]," *IEEE Power and Energy Magazine*, vol.12, no.2, pp.76-96, March-April 2014.
- [2] K. R. Padiyar, HVDC Power Transmission System, Technology and System Interaction, Wiley Eastern Limited, India, 1990.
- [3] J. Arrillaga, Y. H. Liu and N. R. Waston, *Flexible Power Transmission, The HVDC Option*, John Wiley & Sons, Ltd, Chichester, UK, 2007.
- [4] R. Rudervall, J. Charpentier and R. Sharma, "High Voltage Direct Current (HVDC) Transmission Systems Technology Review Paper", *Energy Week 2000, Washington, D.C, USA*, 2000.
- [5] C. Bajracharya, M. Molinas and J. Suul, "Understanding of tuning techniques of converter controllers for VSC-HVDC", *NORPIE/2008, Nordic Workshop on Power and Industrial Electronics, June 9-11, 2008*.



- [6] B. Singh, S. Gairola, B.N. Singh, A. Chandra, K. Al-Haddad, "Multipulse AC–DC Converters for Improving Power Quality: A Review," *IEEE Trans Power Electron*, vol.23, no.1, pp.260-281, Jan. 2008.
- [7] R. Agarwal and S. Singh, "Harmonic Mitigation in Voltage Source Converters based HVDC system Using 12-Pulse AC-DC Converters", in *Annual IEEE India Conference (INDICON)*, 2014.
- [8] D. Madhan Mohan, B. Singh, B.K. Panigrahi, "Harmonic optimised 24- pulse voltage source converter for high voltage DC systems," *IET Power Electronics*, vol.2, no.5, pp.563-573, Sept. 2009.
- [9] S. Singh, B. Singh, "Passive filter design for a 12-pulse converter fedLCI-synchronous motor drive," in *Proc. IEEE PEDES*, 2010, pp.1-8.
- [10] D. M. Mohan, B. Singh, K. B. Panigrahi, "Analysis and design of threelevel, 24-pulse double bridge Voltage Source Converter based HVDC system for active and reactive power control," in *Proc. IEEE PEDES*, pp.1-7, 2010.
- [11] A. A. Rockhill, M. Liserre, R. Teodorescu, and P. Rodriguez, "Grid-filter design for a multimegawatt medium-voltage voltage-source inverter," *IEEE Trans. Ind. Electron.*, vol. 58, no. 4, pp. 1205–1217, Apr. 2011.
- [12] P. Channegowda and V. John, "Filter optimization for grid interactive voltage source inverters," *IEEE Trans. Ind. Electron.*, vol. 57, no. 12, pp. 4106–4114, Dec. 2010.
- [13] B. Misra, B. K. Nayak, "Performance Analysis of Hybrid Filters in High Power Applications", *2nd International Conference on Contemporary Computing and Informatics (ic3i)*, pp. 330-335, 2016.
- [14] R. Beres, X. Wang, F. Blaabjerg, C. Bak, M. Liserre, "A review of passive filters for grid-connected voltage source converters". In: *Applied Power Electronics Conference and Exposition (APEC), 2014 Twenty-Ninth Annual IEEE*, pp. 2208–2215, 2014.
- [15] Klempka R., *A New Method for the C-Type Passive Filter Design*. *Electrical Review* 7a, pp. 277-281.
- [16] P. Li and Q. Hao, "The algorithm for the parameters of AC filters in HVDC transmission system", in *2008 IEEE/PES Transmission and Distribution Conference and Exposition*, Chicago, IL, 2008, pp. 1 - 6.
- [17] B. Badrzadeh, K. Smith and R. Wilson, "Designing Passive Harmonic Filters for an Aluminum Smelting Plant", *IEEE Transactions on Industry Applications*, vol. 47, no. 2, pp. 973-983, 2011.